This article has been accepted for inclusion in a future issue of this journal. Content is final as presented, with the exception of pagination.

Model Predictive Fault-Tolerant Tracking Control for PDF Control Systems With Packet Losses

Lifan Li, *Student Member, IEEE*, Lina Yao, *Member, IEEE*, and Hong Wang, *Senior Member, IEEE*

***Abstract*—In this article, a fault-tolerant tracking control strategy is investigated for nonlinear probability density function (PDF) control systems with the actuator fault, uncertainties, unknown disturbance, and random packet losses. The control input signal dropout and measurement signal dropouts are described as the independent Bernoulli distribution. An adaptive fault diagnosis (FD) observer based on the Lyapunov function is given to simultaneously estimate the fault, disturbance, and state with packet losses. Different from the traditional robust fault-tolerant control (FTC), a new active fault-tolerant tracking controller is designed based on the model predictive control framework, which has better adaptive fault-tolerant performance. Finally, the validity of the proposed FTC method has been proved by a simulation study of a papermaking process.**

***Index Terms*—Fault-tolerant tracking control, model predictive control, probability density function, random packet losses.**

I. Introduction

FOR SOME stochastic systems, in many cases, the control objective is to control the shape of the PDF of the system output rather than the system output signal which is only a function of time. Examples are the particle size distribution control [1] in many geotechnical areas, the molecular weight distribution control of polymer in chemical processes [2], [3], the temperature field distribution control in combustion processes [4], and the fiber length distribution control in refining processes in papermaking [5], [6]. To this end, the stochastic distribution control (SDC) theory [7] with the output PDF as a new research and control objective is proposed by Prof. Hong Wang in 1996. Presently, many research achievements have been obtained for SDC systems in terms of system modeling and control methods [1], [8]–[10]. With the ever increased demand for safety and reliability of the system, research on FD and FTC for stochastic distribution systems has attracted wide attentions. The design of fault-tolerant controller for stochastic distribution control systems has been carried out in two cases: 1) the target PDF is known and 2) the target PDF is unknown. For SDC systems with known target PDF, the design of FTC is to make the output PDF of the post-fault system still track the target one [11], [12]. For SDC systems without known target PDF, the goal of FTC is to minimize the impact of the fault and randomness to the output variables when fault occurs [13], [14].

On the other hand, networked control emerges with the rapid development of computer network and information technique. The industrial applications of SDC systems have entered a new stage of networked control. Indeed, the SDC systems in [2]–[6] are generally controlled by distributed control systems known as DCS, which is a multiple-layered structure with networked communications among each layer and also within the components inside each layer. Due to the intervention of the network, network delay, data packet dropout, multipacket transmission, and other disadvantageous factors were induced [15]. Data packet dropout is one of the main problems that deteriorates the control performance of the system and makes FD and FTC problems [16]–[20] more complicated and challenging. In [19], the quasi-Kalman FD observer was designed and the self-triggered FTC method was established for networked control systems. In addition, nonlinearity is ubiquitous in practical systems, and it is also a challenging problem for FD and FTC of stochastic systems.

For traditional control systems, many FD and FTC techniques have been studied [21], [22]. The FD strategy based on a new intermediate observer was studied for nonlinear multiagent systems in [23]. For fuzzy switched stochastic systems with faults [24], the modified proportional–integral observer was designed to obtain better FD results and the FTC scheme based on estimation information was presented. As a result, some traditional FD and FTC theories and methods are no longer applicable to these stochastic distribution networked control systems with strong non-Gaussian distribution characteristics. Different control algorithms have been studied to achieve the precise tracking control for some complicated systems, such as neural network (NN) control [25], [26], optimal control [27], model predictive control (MPC) [28], and so on. Among them, model predictive control is a promising control algorithm based on the characteristics and requirements of industrial process control. The control sequence of model predictive control was obtained by solving an optimization problem which minimizes the objective function

Manuscript received September 26, 2020; revised April 25, 2021; accepted July 31, 2021. This work was supported by UT-Battelle, LLC, under Contract DE-AC05-00OR22725 with the U.S. Department of Energy (DOE). The work of Lifan Li and Lina Yao was supported in part by the National Natural Science Foundation of China under Grant 61973278, and in part by the Basic Research Projects of Key Scientific Research Projects of Colleges and Universities in Henan under Grant 21zx007. This article was recommended by Associate Editor Y. Song. *(Corresponding author: Lina Yao.)*

Lifan Li and Lina Yao are with the School of Electrical Engineering, Zhengzhou University, Zhengzhou 450001, China (e-mail: michelle_lnxq@126.com).

Hong Wang was with the Institute of Science and Technology, University of Manchester, Manchester M13 9PL, U.K. He is now with the Energy and Transportation Science Division, Oak Ridge National Laboratory, Oak Ridge, TN 37934 USA.

Color versions of one or more figures in this article are available at https://doi.org/10.1109/TSMC.2021.3103814.

Digital Object Identifier 10.1109/TSMC.2021.3103814

2168-2216 © 2021 IEEE. Personal use is permitted, but republication/redistribution requires IEEE permission.
See https://www.ieee.org/publications/rights/index.html for more information.

Authorized licensed use limited to: Oak Ridge National Laboratory. Downloaded on August 22,2021 at 17:47:03 UTC from IEEE Xplore. Restrictions apply.

This article has been accepted for inclusion in a future issue of this journal. Content is final as presented, with the exception of pagination.

at each sampling time [29]. It has been shown that MPC can be used to effectively deal with uncertainties, nonlinearities, and constraints in networked control systems [30]. At the same time, MPC is also used to solve the problem of FTC. For example, a new algorithm for designing robust fault-tolerant explicit model predictive controller was derived for the uncertain system with disturbances and actuator fault in [31]. In order to solve the intermittent actuator fault in large-scale systems, a cooperative distributed fault-tolerant control based on the MPC scheme was proposed [32]. This indicates that it is of great significance to solve the problem of FTC for PDF control systems with packet losses by using the model predictive control framework. However, the related research has not been much reported to the best of our knowledge, which motivates our work.

According to the above discussions and analysis, we attempt to deal with the fault-tolerant tracking control problem for Lipschitz nonlinear PDF control systems in the presence of packet losses and actuator fault. Compared with the existing research on FTC of PDF control systems, the main contents and contributions can be summarized as follows.

1) A novel FD and fault-tolerant tracking control strategy considering the actuator fault, uncertainties, unknown disturbance, and random packet losses is first proposed for the nonlinear PDF control system. In the presence of random packet losses, the fault-tolerant tracking control design for PDF control systems becomes much more difficult. It should be noted that both control input signal dropouts and measurement signal dropouts are considered in the PDF control system.
2) Compared with the existing FD method, the weighted integral of the error of the output PDF is introduced as the residual signal in the design of the observer. In case of packet losses in the system, the actuator fault and disturbance are estimated simultaneously. In particular, the fault whose size changes frequently can also be accurately estimated.
3) Different from the traditional robust fault-tolerant control, the model predictive fault-tolerant tracking controller based on the estimated information is designed to compensate the impact of fault on the system.

The organization of the remainder of this article is as follows. The description of the nonlinear PDF control with packet losses is shown in Section II. The design of the FD algorithm and the stability proof of the error dynamic system are given in Section III. In Section IV, by using the estimated information and MPC, the fault-tolerant tracking controller is described. Section V gives the simulation results. Finally, conclusions are given in Section VI.

II. System Model Description

The establishment of the PDF control system includes the static model and the dynamic model. For the nonlinear PDF control system, by using linear B-spline approximation [8], [33], the instant approximation to the output PDF $\gamma_k(y, u_k)$ can be expressed as follows:

$$\gamma_k(y, u_k) = \sum_{s=1}^{N} \omega_s(u_k)\varphi_s(y) + \omega_0(y, u_k) \tag{1}$$

where u_k denotes the input of the PDF control system and the random output variable y of the system defined on the domain $[a, b]$ is continuous and bounded. $\omega_s(u_k)(s = 1, 2, \ldots, N)$ denote the corresponding dynamic weights associated with the control input, and $\varphi_s(y)(s = 1, 2, \ldots, N)$ are the predetermined basis functions. $\omega_0(y, u_k)$ denotes the approximate error of the output PDF and satisfies the condition that $\|\omega_0(y, u_k)\| \leq \varsigma$, which is a small upper bound of the approximation error.

Since $\gamma_k(y, u_k)$ is the output PDF defined on the certain interval $[a, b]$, the condition that $\int_a^b \gamma_k(y, u_k)dy = 1$ must be satisfied. Define $\phi^T = (\phi_1, \phi_2, \ldots, \phi_{N-1}) \in R^{N-1}, \phi_s = \int_a^b \varphi_s(y)dy$, (1) can be further rewritten as follows:

$$\gamma_k(y, u_k) = \varphi(y)w_k + \psi(y) + \omega_0(y, u_k) \tag{2}$$

where $\varphi(y) = \varphi_0(y) - ([\varphi_N(y)]/\phi_N)\phi^T$, $\psi(y) = ([\varphi_N(y)]/\phi_N)$, $\varphi_0(y) = [\varphi_1(y), \ldots, \varphi_{N-1}(y)] \in R^{1\times(N-1)}, w_k = [\omega_1(u_k), \ldots, \omega_{N-1}(u_k)]^T \in R^{N-1}$. In what follows, $\gamma_k(y, u_k)$ will be abbreviated as γ_k.

Remark 1: The mathematical model of PDF is usually obtained by the partial differential equation theory. However, it is generally difficult to obtain the accurate partial differential equation expression in practical applications, and usually, only the distribution samples can be obtained. Therefore, it is necessary to establish a static model of a non-Gaussian stochastic distribution system, that is, to use linear B-spline to approximate the instant PDF. The output PDF is approximated by the linear function relationship between the predetermined basis functions and the output weight vector in this article, whose form is given by system (1). The dynamic model between the control input and the weight vector is established by using the identification method [7]. The purpose of establishing the static model and the dynamic model is to transform the shape control of the output PDF into the control of the weight vector.

The following Lipschitz nonlinear dynamic model that links the weights in (1) with the control input for the PDF control system is considered as:

$$x_{k+1} = (A + \Delta A)x_k + (B + \Delta B)u_k + g(x_k) + Hf_k + D_0d_k \tag{3}$$

$$w_k = Dx_k \tag{4}$$

where $x_k \in R^n$ denotes the state vector and f_k denotes the additive fault vector. A, B, H, D_0, and D are known system parameter matrices with appropriate dimensions. ΔA and ΔB are the parametric uncertainties, which can be described in the following form:

$$\begin{bmatrix} \Delta A & \Delta B \end{bmatrix} = F\varpi_k \begin{bmatrix} H_1 & H_2 \end{bmatrix}$$

where F, H_1, and H_2 are known constant matrices, and ϖ_k is the time-varying matrix which satisfies $\varpi_k^T\varpi_k \leq I$.

The unknown external disturbance d_k is supposed to be described by an exogenous system [34] as follows:

$$\begin{cases} \delta_{k+1} = C\delta_k \\ d_k = V\delta_k \end{cases} \tag{5}$$

Authorized licensed use limited to: Oak Ridge National Laboratory. Downloaded on August 22,2021 at 17:47:03 UTC from IEEE Xplore. Restrictions apply.

This article has been accepted for inclusion in a future issue of this journal. Content is final as presented, with the exception of pagination.

where $\delta_k \in R^q$ is the state of the exogenous system, and C and V are known matrices with appropriate dimensions. Model (5) is a so-called autonomous system without considering the external excitation signal [35], which can be used to describe constant disturbances and harmonic disturbances with unknown amplitude and phase.

In (3), $g(x_k)$ is a nonlinear function satisfying $g(0) = 0$ and the following Lipschitz condition:

$$\|g(x_{1k}) - g(x_{2k})\| \le \lambda \|x_{1k} - x_{2k}\| \quad \forall x_{1k}, x_{2k} \in R^n \tag{6}$$

where λ is a positive scalar.

The loss of control signal and measurement data is inevitable because of the features of network. Here, we introduce two random variables $\alpha_k \in \{0, 1\}$ and $\beta_k \in \{0, 1\}$ which are the independent Bernoulli distributed white sequences. They are introduced to model the loss of the control signal and missing measurements [19], respectively. $\alpha_k = 1$ and $\beta_k = 1$ mean that the output PDF γ_k and the input u_k are successfully transmitted. However, $\alpha_k = 0$ and $\beta_k = 0$ indicate that the output PDF γ_k and the input u_k are unsuccessfully transmitted.

When the packet loss occurs at time k, the latest available packet at time $k-1$ will be used for the compensation for the feedback control realization. Thus, we have

$$\bar{\gamma}_k = \alpha_k \gamma_k + (1 - \alpha_k)\bar{\gamma}_{k-1}, \quad \bar{u}_k = \beta_k u_k + (1 - \beta_k)\bar{u}_{k-1} \tag{7}$$

where α_k and β_k obey the Bernoulli distribution with $\text{Prob}\{\alpha_k = 1\} = \text{E}\{\alpha_k\} = \bar{\alpha}$, $\text{var}\{\alpha_k\} = \text{E}\{(\alpha_k - \bar{\alpha})^2\} = \tilde{\alpha}^2$, $\text{Prob}\{\beta_k = 1\} = \text{E}\{\beta_k\} = \bar{\beta}$, and $\text{var}\{\beta_k\} = \text{E}\{(\beta_k - \bar{\beta})^2\} = \tilde{\beta}^2$, where $\bar{\alpha}$ and $\bar{\beta}$ are the expected value of α_k and β_k, respectively. $\tilde{\alpha}^2$ is the variance of α_k and $\tilde{\beta}^2$ is the variance of β_k. The purpose of the FTC design is to: 1) make use of the available input and output PDF of the system to carry out effective fault diagnosis considering possible packet losses and 2) design the FTC strategy based on model predictive control so that the system can still operate safely when the fault occurs.

III. Fault Diagnosis

The results of fault estimation directly affect the performance of fault-tolerant control. In this section, fault diagnosis for systems (1)–(7) will be described. For this purpose, define a new state vector $z_k = \begin{bmatrix} x_k \\ \delta_k \end{bmatrix}$, the augmented system that integrates (2)–(7) can be described as follows:

$$z_{k+1} = \big(\bar{A} + \Delta\bar{A}\big)z_k + \big(\bar{B} + \Delta\bar{B}\big)\bar{u}_k + \bar{I}g(z_k) + \bar{H}f_k \tag{8}$$

$$w_k = \bar{D}z_k \tag{9}$$

where $\bar{A} = \begin{bmatrix} A & D_0 V \\ 0 & C \end{bmatrix}$, $\Delta\bar{A} = \begin{bmatrix} \Delta A & 0 \\ 0 & 0 \end{bmatrix}$, $\bar{B} = \begin{bmatrix} B \\ 0 \end{bmatrix}$, $\Delta\bar{B} = \begin{bmatrix} \Delta B \\ 0 \end{bmatrix}$, $\bar{I} = \begin{bmatrix} I & 0 \\ 0 & 0 \end{bmatrix}$, $\bar{H} = \begin{bmatrix} H \\ 0 \end{bmatrix}$, $\bar{D} = \begin{bmatrix} D & 0 \end{bmatrix}$.

The following fault estimation observer is given to diagnose the fault:

$$\hat{z}_{k+1} = \bar{A}\hat{z}_k + \bar{B}\bar{u}_k + \bar{H}\hat{f}_k + L\varepsilon_k + \bar{I}g\big(\hat{z}_k\big) \tag{10}$$

$$\hat{w}_k = \bar{D}\hat{z}_k \tag{11}$$

$$\hat{\gamma}_k = \bar{\alpha}\hat{\gamma}_k + (1 - \bar{\alpha})\hat{\gamma}_{k-1} \tag{12}$$

$$\hat{f}_{k+1} = \hat{f}_k + \Gamma\varepsilon_k \tag{13}$$

where $\hat{z}_k$ denotes the state estimation vector of the augmented system, $\hat{w}_k$ denotes the estimation of w_k, $\hat{\gamma}_k$ denotes the estimation of γ_k, and $\hat{f}_k$ is defined as the estimation of f_k. L is defined as the adaptive gain and Γ is the learning operator to be determined later. ε_k is the residual which is expressed as follows:

$$\varepsilon_k = \int_a^b \sigma(y)\big(\bar{\gamma}_k - \hat{\gamma}_k\big)dy \tag{14}$$

where $\sigma(y)$ is a predetermined factor [7].

Denote the state estimation error vector e_k and the fault estimation error vector $\tilde{f}_k$ as follows:

$$e_k = z_k - \hat{z}_k, \quad \tilde{f}_k = f_k - \hat{f}_k. \tag{15}$$

ε_k can be represented as follows:

$$\begin{aligned}\varepsilon_k &= \int_a^b \sigma(y)\varphi(y)dy\big(\alpha_k\bar{D}z_k + (1-\alpha_k)\bar{D}z_{k-1} - \bar{\alpha}\bar{D}\hat{z}_k \\ &\qquad - (1-\bar{\alpha})\bar{D}\hat{z}_{k-1} + (1-\alpha_k)\tilde{w}_{k-1}\big) \\ &\quad + \int_a^b \sigma(y)\omega_0(y, u_k)dy \\ &= \Sigma\big((\alpha_k - \bar{\alpha})\bar{D}\Delta z_k + \bar{\alpha}\bar{D}e_k + (1-\bar{\alpha})\bar{D}e_{k-1} \\ &\qquad + (1-\alpha_k)\tilde{w}_{k-1}\big) + \rho_k\end{aligned} \tag{16}$$

where $\Sigma = \int_a^b \sigma(y)\varphi(y)dy$, $\tilde{w}_{k-1} = \bar{w}_{k-1} - w_{k-1}$, and $\rho_k = \int_a^b \sigma(y)\omega_0(y, u_k)dy$. It is easy to obtain that $\|\rho_k\| \le \tilde{\varsigma}$, where $\tilde{\varsigma} = \varsigma\|\int_a^b \sigma(y)dy\|$.

Using the system and the observer models, it can be further obtained that

$$\begin{aligned}e_{k+1} &= \big(\bar{A} - L\Sigma\bar{\alpha}\bar{D}\big)e_k - L\Sigma(1-\bar{\alpha})\bar{D}e_{k-1} + \bar{I}\Delta G_k \\ &\quad + \bar{H}\tilde{f}_k - L\Sigma(\alpha_k - \bar{\alpha})\bar{D}\Delta z_k + \Delta\bar{A}z_k \\ &\quad + \Delta\bar{B}u_k - L\rho_k - L\Sigma(1-\alpha_k)\tilde{w}_{k-1} \\ &= \big(\bar{A} - L\Sigma\bar{\alpha}\bar{D}\big)e_k - L\Sigma(1-\bar{\alpha})\bar{D}e_{k-1} + \bar{I}\Delta G_k \\ &\quad + \bar{H}\tilde{f}_k - L\Sigma(\alpha_k - \bar{\alpha})\bar{D}\Delta z_k + D_1\upsilon_k\end{aligned} \tag{17}$$

$$\begin{aligned}\tilde{f}_{k+1} &= f_{k+1} - f_k + \tilde{f}_k \\ &\quad - \Gamma\big(\Sigma\big((\alpha_k - \bar{\alpha})\bar{D}\Delta z_k + \bar{\alpha}\bar{D}e_k + (1-\bar{\alpha})\bar{D}e_{k-1}\big)\big) \\ &\quad - \Gamma\rho_k - \Gamma\Sigma(1-\alpha_k)\tilde{w}_{k-1} \\ &= \tilde{f}_k - (\alpha_k - \bar{\alpha})\Gamma\Sigma\bar{D}\Delta z_k - \bar{\alpha}\Gamma\Sigma\bar{D}e_k \\ &\quad - L(1-\bar{\alpha})\Gamma\Sigma\bar{D}e_{k-1} + D_2\upsilon_k\end{aligned} \tag{18}$$

where it has been denoted that

$$\begin{aligned}\Delta G_k &= g(z_k) - g\big(\hat{z}_k\big) \\ D_1 &= \begin{bmatrix} \Delta\bar{A} & \Delta\bar{B} & -L & -L\Sigma(1-\alpha_k) & 0 & 0 & 0 \end{bmatrix} \\ D_2 &= \begin{bmatrix} 0 & 0 & -\Gamma & -\Gamma\Sigma(1-\alpha_k) & I & 0 & 0 \end{bmatrix} \\ \upsilon_k &= \begin{bmatrix} z_k & u_k & \rho_k & \tilde{w}_{k-1} & \Delta f_{k+1} & \Delta u_k & \Delta f_k \end{bmatrix}^T \\ \Delta f_{k+1} &= f_{k+1} - f_k.\end{aligned}$$

According to (7) and (8), the incremental discrete model is described as follows:

$$\begin{aligned}\Delta z_{k+1} &= \bar{A}\Delta z_k + \bar{B}\beta_k\Delta u_k + \bar{H}\Delta f_k + \bar{I}(g(z_k) - g(z_{k-1})) \\ &\quad + \Delta\bar{A}_k z_k - \Delta\bar{A}_{k-1}z_{k-1} + \Delta\bar{B}_k\bar{u}_k - \Delta\bar{B}_{k-1}\bar{u}_{k-1}\end{aligned} \tag{19}$$

Authorized licensed use limited to: Oak Ridge National Laboratory. Downloaded on August 22,2021 at 17:47:03 UTC from IEEE Xplore. Restrictions apply.

This article has been accepted for inclusion in a future issue of this journal. Content is final as presented, with the exception of pagination.

where $\Delta z_{k+1} = z_{k+1} - z_k$ is the state increment of the augmented system, $\Delta u_k = \bar{u}_k - \bar{u}_{k-1}$ is the input increment, $\Delta g_k = g(z_k) - g(z_{k-1})$ is the nonlinear increment of the augmented system, and $\Delta f_k = f_k - f_{k-1}$ is the fault increment.

When the sampling period is small enough, the increment caused by the parametric uncertainties [36] can be ignored, which can be described as follows:

$$\begin{cases} \Delta\bar{A}_k z_k - \Delta\bar{A}_{k-1} z_{k-1} \approx 0 \\ \Delta\bar{B}_k \bar{u}_k - \Delta\bar{B}_{k-1}\bar{u}_{k-1} \approx 0. \end{cases}$$

Therefore, the incremental discrete model (19) can be simplified as follows:

$$\Delta z_{k+1} = \bar{A}\Delta z_k + \bar{I}\Delta g_k + D_3 \upsilon_k \tag{20}$$

where $D_3 = \begin{bmatrix} 0 & 0 & 0 & 0 & 0 & \bar{B}\beta_k & \bar{H} \end{bmatrix}$.

Assumption 1: It is supposed that the fault increment Δf_k and the control increment Δu_k are bounded [37], [38], the following conditions are satisfied:

$$\|\Delta f_k\| \le a_1, \|\Delta u_k\| \le a_2$$

where a_1 and a_2 are positive constants.

Lemma 1 (S-Procedure [39]): Set $T_i \in R^{n\times n}(i = 0, 1, \ldots, l)$ are symmetric matrices. The conditions that $\xi^T T_0 \xi \ge 0 \ \forall \xi \ne 0 \ \ s.t. \ \ \xi^T T_i \xi \ge 0 (i = 1, \ldots, l)$ is established if there exist $\tau_i \ge 0 (i = 0, 1, \ldots, l)$ such that $T_0 - \sum_{i=1}^{l} \tau_i T_i \ge 0$.

Lemma 2 [40]: Let $\tilde{F}$ and $\tilde{H}$ be real matrices with appropriate dimension and ϖ_k satisfies $\varpi_k^T \varpi_k \le I$. Then, for any positive constant $\varepsilon > 0$, the following inequality is true:

$$\tilde{H}^T \varpi_k^T \tilde{F}^T + \tilde{F}\varpi_k \tilde{H} \le \varepsilon^{-1}\tilde{H}^T\tilde{H} + \varepsilon \tilde{F}\tilde{F}^T.$$

Remark 2: Due to the natural conditions in all physical systems, it is clear that the performance of the actuator is limited. Considering this unavoidable performance constraint, it is reasonable to assume that Δf_k and Δu_k are bounded.

Theorem 1: For the parameter $\kappa > 0$, it is supposed that there exist matrices $P_1 = P_1^T > 0$, $P_2 = P_2^T > 0$, $P_3 = P_3^T > 0$, $P_4 = P_4^T > 0, R_1$, R_2 and positive real scalars $\tau_1 \ge 0, \tau_2 \ge 0$ such that the following LMI:

$$\begin{bmatrix} \Omega^1 & \Omega^2 \\ * & \Omega^3 \end{bmatrix} < 0 \tag{21}$$

holds, where

$$\Omega^1 = \mathrm{diag}\left\{\Omega_{11}^1, \Omega_{22}^1, \Omega_{33}^1, \Omega_{44}^1, \Omega_{55}^1, \Omega_{66}^1, \Omega_{77}^1\right\}$$
$$\Omega_{11}^1 = -P_1 + I - \tau_1\lambda^2 I, \Omega_{22}^1 = -P_2$$
$$\Omega_{33}^1 = -P_3, \Omega_{44}^1 = -\tau_1 I$$
$$\Omega_{55}^1 = -P_4 - \tau_2\lambda^2 I, \Omega_{66}^1 = -\tau_2 I, \Omega_{77}^1 = -\kappa^2 I + 2\varepsilon^{-1}\widehat{H}^T\widehat{H}$$
$$\Omega^2 = \begin{bmatrix} \Omega_{11}^2 & P_2 & \Omega_{13}^2 & 0 & 0 & 0 & 0 \\ \Omega_{21}^2 & 0 & \Omega_{23}^2 & 0 & 0 & 0 & 0 \\ \Omega_{31}^2 & 0 & P_3 & 0 & 0 & 0 & 0 \\ \Omega_{41}^2 & 0 & 0 & 0 & 0 & 0 & 0 \\ 0 & 0 & 0 & \Omega_{54}^2 & \Omega_{55}^2 & \Omega_{56}^2 & 0 \\ 0 & 0 & 0 & 0 & 0 & \Omega_{66}^2 & 0 \\ \Omega_{71}^2 & 0 & 0 & \Omega_{74}^2 & \Omega_{75}^2 & \Omega_{76}^2 & 0 \end{bmatrix}$$
$$\Omega_{11}^2 = \bar{A}^T P_1 - \bar{\alpha}\bar{D}^T\Sigma^T R_1^T, \Omega_{13}^2 = -\bar{\alpha}\bar{D}^T\Sigma^T R_2^T$$
$$\Omega_{21}^2 = -(1-\bar{\alpha})\bar{D}^T\Sigma^T R_1^T, \Omega_{23}^2 = (1-\bar{\alpha})\bar{D}^T\Sigma^T R_2^T$$
$$\Omega_{31}^2 = \bar{H}^T P_1, \Omega_{41}^2 = \bar{I}^T P_1, \Omega_{54}^2 = \bar{\alpha}\bar{D}^T\Sigma^T R_1^T$$
$$\Omega_{55}^2 = \tilde{\alpha}\bar{D}^T\Sigma^T R_2^T, \Omega_{56}^2 = \bar{A}^T P_4, \Omega_{66}^2 = \bar{I}^T P_4$$
$$\Omega_{71}^2 = \Omega_{74}^2 = \begin{bmatrix} 0 & 0 & -R_1 & 0 & 0 & 0 \end{bmatrix}^T$$
$$\Omega_{75}^2 = \begin{bmatrix} 0 & 0 & -R_2 & P_3 & 0 & 0 \end{bmatrix}^T$$
$$\Omega_{76}^2 = \begin{bmatrix} 0 & 0 & 0 & 0 & \bar{B}\bar{\beta}P_4 & \bar{H}P_4 \end{bmatrix}^T$$
$$\Omega^3 = \begin{bmatrix} \Omega_{11}^3 & \Omega_{12}^3 \\ 0 & -\varepsilon I \end{bmatrix}$$
$$\Omega_{11}^3 = \mathrm{diag}\{-P_1, -P_2, -P_3, -P_1, -P_3, -P_3\}$$
$$\Omega_{12}^3 = \begin{bmatrix} P_1\widehat{F} & 0 & 0 & P_1\widehat{F} & 0 & 0 \end{bmatrix}^T$$
$$L = P_1^{-1}R_1, \Gamma = P_3^{-1}R_2.$$

Then, the error dynamic system (17) is stable and satisfies the H_∞ performance index $\sum_{k=0}^{\infty}\mathrm{E}\|e_k\|^2 \le \kappa^2\sum_{k=0}^{\infty}\mathrm{E}\|\upsilon_k\|^2$ when the adaptive fault diagnosis observer (10)–(13) is used.

Proof: Define a Lyapunov function as follows:

$$\pi_k = e_k^T P_1 e_k + e_{k-1}^T P_2 e_{k-1} + \tilde{f}_k^T P_3 \tilde{f}_k + \Delta z_k^T P_4 \Delta z_k. \tag{22}$$

Then, it can be obtained that

$$\begin{aligned}
&\mathrm{E}\{\pi_{k+1} - \pi_k\} + \mathrm{E}\left\{e_k^T e_k\right\} - \kappa^2 \mathrm{E}\left\{\upsilon_k^T \upsilon_k\right\} \\
&= \mathrm{E}\Big\{e_{k+1}^T P_1 e_{k+1} + e_k^T P_2 e_k + \tilde{f}_{k+1}^T P_3 \tilde{f}_{k+1} \\
&\qquad + \Delta z_{k+1}^T P_4 \Delta z_{k+1} - e_k^T P_1 e_k - e_{k-1}^T P_2 e_{k-1} \\
&\qquad - \tilde{f}_k^T P_3 \tilde{f}_k - \Delta z_k^T P_4 \Delta z_k + e_k^T e_k - \kappa^2 \upsilon_k^T \upsilon_k\Big\} \\
&= \mathrm{E}\Big\{\Big[\big(\bar{A} - L\Sigma\bar{\alpha}\bar{D}\big)e_k - L\Sigma(1-\bar{\alpha})\bar{D}e_{k-1} + \bar{I}\Delta G_k \\
&\qquad + \bar{H}\tilde{f}_k - L\Sigma(\alpha_k - \bar{\alpha})\bar{D}\Delta z_k + D_1\upsilon_k\Big]^T P_1 \\
&\qquad \Big[\big(\bar{A} - L\Sigma\bar{\alpha}\bar{D}\big)e_k - L\Sigma(1-\bar{\alpha})\bar{D}e_{k-1} + \bar{I}\Delta G_k \\
&\qquad + \bar{H}\tilde{f}_k - L\Sigma(\alpha_k - \bar{\alpha})\bar{D}\Delta z_k + D_1\upsilon_k\Big] + e_k^T P_2 e_k \\
&\qquad + \Big[\tilde{f}_k - \Gamma\Sigma\big((\alpha_k - \bar{\alpha})\bar{D}\Delta z_k + \bar{\alpha}\bar{D}e_k \\
&\qquad\qquad + (1-\bar{\alpha})\bar{D}e_{k-1}\big) + D_2\upsilon_k\Big]^T \\
&\qquad P_3\Big[\tilde{f}_k - \Gamma\Sigma((\alpha_k - \bar{\alpha})D\Delta z_k + \bar{\alpha}De_k \\
&\qquad\qquad + (1-\bar{\alpha})De_{k-1}) + D_2\upsilon_k\Big] \\
&\qquad + \left[\bar{A}\Delta z_k + \bar{I}\Delta g_k + D_3\upsilon_k\right]^T P_4 \\
&\qquad \left[\bar{A}\Delta z_k + \bar{I}\Delta g_k + D_3\upsilon_k\right] - e_k^T P_1 e_k - e_{k-1}^T P_2 e_{k-1} \\
&\qquad - \tilde{f}_k^T P_3 \tilde{f}_k - \Delta z_k^T P_4 \Delta z_k + e_k^T e_k - \kappa^2 \upsilon_k^T \upsilon_k\Big\} \\
&= \bar{e}_k^T \Phi_1 \bar{e}_k
\end{aligned} \tag{23}$$

where

$$\bar{e}_k^T = \begin{bmatrix} e_k^T & e_{k-1}^T & \tilde{f}_k^T & \Delta G_k^T & \Delta z_k^T & \Delta g_k^T & \upsilon_k^T \end{bmatrix}$$

Authorized licensed use limited to: Oak Ridge National Laboratory. Downloaded on August 22,2021 at 17:47:03 UTC from IEEE Xplore. Restrictions apply.

This article has been accepted for inclusion in a future issue of this journal. Content is final as presented, with the exception of pagination.

$$\Phi_1 = \begin{bmatrix} \Phi_{111} & \Phi_{112} & \Phi_{113} & \Phi_{114} & 0 & 0 & \Phi_{117} \\ * & \Phi_{122} & \Phi_{123} & \Phi_{124} & 0 & 0 & \Phi_{127} \\ * & * & \Phi_{133} & \Phi_{134} & 0 & 0 & \Phi_{137} \\ * & * & * & \Phi_{144} & 0 & 0 & \Phi_{147} \\ * & * & * & * & \Phi_{155} & \Phi_{156} & \Phi_{157} \\ * & * & * & * & * & \Phi_{166} & \Phi_{167} \\ * & * & * & * & * & * & \Phi_{177} \end{bmatrix}$$

$$\begin{aligned}
\Phi_{111} &= \big(\bar{A} - L\Sigma\bar{\alpha}\bar{D}\big)^T P_1\big(\bar{A} - L\Sigma\bar{\alpha}\bar{D}\big) + P_2 \\
&\quad + \big(\Gamma\Sigma\bar{\alpha}\bar{D}\big)^T P_3\Gamma\Sigma\bar{\alpha}\bar{D} - P_1 + I \\
\Phi_{112} &= -\big(\bar{A} - L\Sigma\bar{\alpha}\bar{D}\big)^T P_1\big(L\Sigma(1-\bar{\alpha})\bar{D}\big) \\
&\quad + \big(\Gamma\Sigma\bar{\alpha}\bar{D}\big)^T P_3\big(\Gamma\Sigma(1-\bar{\alpha})\bar{D}\big) \\
\Phi_{113} &= \big(\bar{A} - L\Sigma\bar{\alpha}\bar{D}\big)^T P_1\bar{H} - \big(\Gamma\Sigma\bar{\alpha}\bar{D}\big)^T P_3 \\
\Phi_{114} &= \big(\bar{A} - L\Sigma\bar{\alpha}\bar{D}\big)^T P_1\bar{I} \\
\Phi_{117} &= \big(\bar{A} - L\Sigma\bar{\alpha}\bar{D}\big)^T P_1 D_1 - \big(\Gamma\Sigma\bar{\alpha}\bar{D}\big)^T P_3 D_2 \\
\Phi_{122} &= \big(L\Sigma(1-\bar{\alpha})\bar{D}\big)^T P_1 L\Sigma(1-\bar{\alpha})\bar{D} \\
&\quad + \big(\Gamma\Sigma(1-\bar{\alpha})\bar{D}\big)^T P_3\Gamma\Sigma(1-\bar{\alpha})\bar{D} - P_2 \\
\Phi_{123} &= -\big(L\Sigma(1-\bar{\alpha})\bar{D}\big)^T P_1\bar{H} - \big(\Gamma\Sigma(1-\bar{\alpha})\bar{D}\big)^T P_3 \\
\Phi_{124} &= -\big(L\Sigma(1-\bar{\alpha})\bar{D}\big)^T P_1\bar{I} \\
\Phi_{127} &= -\big(L\Sigma(1-\bar{\alpha})\bar{D}\big)^T P_1 D_1 - \big(\Gamma\Sigma(1-\bar{\alpha})\bar{D}\big)^T P_3 D_2 \\
\Phi_{133} &= \bar{H}^T P_1\bar{H},\ \Phi_{134} = \bar{H}^T P_1\bar{I},\ \Phi_{137} = \bar{H}^T P_1 D_1 + P_3 D_2 \\
\Phi_{144} &= \bar{I}^T P_1\bar{I},\ \Phi_{147} = \bar{I}^T P_1 D_1 \\
\Phi_{155} &= \big(L\Sigma\tilde{\alpha}\bar{D}\big)^T P_1 L\Sigma\tilde{\alpha}\bar{D} + \big(\Gamma\Sigma\tilde{\alpha}\bar{D}\big)^T P_3\Gamma\Sigma\tilde{\alpha}\bar{D} \\
&\quad + \bar{A}^T P_4\bar{A} - P_4 \\
\Phi_{156} &= \bar{A}^T P_4\bar{I},\ \Phi_{157} = \bar{A}^T P_4\bar{D}_3 \\
\Phi_{166} &= \bar{I}^T P_4\bar{I},\ \Phi_{167} = \bar{I}^T P_4\bar{D}_3 \\
\Phi_{177} &= D_1^T P_1 D_1 + D_2^T P_3 D_2 + \bar{D}_3^T P_4\bar{D}_3 - \kappa^2 I \\
D_1 &= D_{11} + D_{12} \\
D_{11} &= \begin{bmatrix} 0 & 0 & -L & 0 & 0 & 0 \end{bmatrix} \\
D_{12} &= \begin{bmatrix} \Delta\bar{A} & \Delta\bar{B} & 0 & 0 & 0 & 0 \end{bmatrix} \\
&= \begin{bmatrix} \Delta A & 0 & \Delta B & 0 & 0 & 0 & 0 \\ 0 & 0 & 0 & 0 & 0 & 0 & 0 \end{bmatrix} \\
&= \begin{bmatrix} F \\ 0 \end{bmatrix}\varpi_k\begin{bmatrix} H_1 & 0 & H_2 & 0 & 0 & 0 & 0 \end{bmatrix} \\
&= \widehat{F}\varpi_k\widehat{H} \\
\bar{D}_3 &= \begin{bmatrix} 0 & 0 & 0 & 0 & \bar{B}\bar{\beta} & \bar{H} \end{bmatrix}.
\end{aligned}$$

According to the Lipschitz condition, it can be obtained that

$$\Delta G_k^T\Delta G_k = \|\Delta G_k\|^2 \le \|\lambda e_k\|^2 = \lambda^2 e_k^T e_k \tag{24}$$

$$\Delta g_k^T\Delta g_k \le \|\lambda\Delta z_k\|^2 = \lambda^2\Delta z_k^T\Delta z_k. \tag{25}$$

Thus, we have

$$\Delta G_k^T\Delta G_k - \lambda^2 e_k^T e_k \triangleq \bar{e}_k^T\Lambda_1\bar{e}_k \le 0 \tag{26}$$

$$\Delta g_k^T\Delta g_k - \lambda^2\Delta z_k^T\Delta z_k \triangleq \bar{e}_k^T\Lambda_2\bar{e}_k \le 0 \tag{27}$$

where

$$\Lambda_1 = \mathrm{diag}\Big\{-\lambda^2 I, 0, 0, I, 0, 0, 0\Big\}$$

$$\Lambda_2 = \mathrm{diag}\Big\{0, 0, 0, 0, -\lambda^2 I, I, 0\Big\}.$$

By using the well-known S-procedure in Lemma 1, $\Phi_1 < 0$ under constraints (24) and (25) hold, if there exist matrices $P_1 = P_1^T > 0$, $P_2 = P_2^T > 0$, $P_3 = P_3^T > 0$, $P_4 = P_4^T > 0$, and positive real scalars $\tau_1 \ge 0$, $\tau_2 \ge 0$ such that

$$\Phi_2 = \Phi_1 - \tau_1\Lambda_1 - \tau_2\Lambda_2 < 0. \tag{28}$$

From Lemma 2, the following inequalities can be obtained:

$$\breve{H}^T\varpi_k\breve{F}_1^T + \breve{F}_1\varpi_k\breve{H}^T \le \varepsilon^{-1}\breve{H}^T\breve{H} + \varepsilon\breve{F}_1\breve{F}_1^T \tag{29}$$

$$\breve{H}^T\varpi_k\breve{F}_2^T + \breve{F}_2\varpi_k\breve{H}^T \le \varepsilon^{-1}\breve{H}^T\breve{H} + \varepsilon\breve{F}_2\breve{F}_2^T \tag{30}$$

where

$$\begin{aligned}
\breve{H} &= \begin{bmatrix} 0 & 0 & 0 & 0 & 0 & 0 & \widehat{H} & 0 & 0 & 0 & 0 & 0 & 0 \end{bmatrix} \\
\breve{F}_1^T &= \begin{bmatrix} 0 & 0 & 0 & 0 & 0 & 0 & 0 & \widehat{F}^T P_1 & 0 & 0 & 0 & 0 & 0 \end{bmatrix} \\
\breve{F}_2^T &= \begin{bmatrix} 0 & 0 & 0 & 0 & 0 & 0 & 0 & 0 & 0 & 0 & \widehat{F}^T P_1 & 0 & 0 \end{bmatrix} \\
\widehat{H} &= \begin{bmatrix} H_1 & 0 & H_2 & 0 & 0 & 0 & 0 \end{bmatrix}, \widehat{F} = \begin{bmatrix} F^T & 0 \end{bmatrix}^T.
\end{aligned}$$

According to the Schur complement lemma and the inequalities (29), (30), it can be obtained that (21) is equivalent to (28). Thus, the following inequality is established:

$$\sum_{k=0}^{\infty}\mathrm{E}\big\{e_k^T e_k\big\} \le \kappa^2\sum_{k=0}^{\infty}\mathrm{E}\big\{\upsilon_k^T\upsilon_k\big\}. \tag{31}$$

Then, it can be guaranteed that the observation error dynamic system is stable and satisfies the H_∞ performance.

Remark 3: By designing an observer for the augmented system, it is easy to obtain that $\hat{x}_k = [I \quad 0]\hat{z}_k, \hat{d}_k = [0 \quad V]\hat{z}_k$, where $\hat{x}_k$ and $\hat{d}_k$ are the state estimation and the disturbance estimation, respectively.

IV. Model Predictive Fault-Tolerant Control

The estimated fault vector is used to reconstruct the controller in this section, so as to guarantee the tracking performance of the post-fault system. The weight value of the desired PDF γ_g is defined as w_g. Then, it can be obtained that $\gamma_g = \varphi(y)w_g + \psi(y)$.

When the following condition:

$$\lim_{k\to\infty}\big(\gamma_g - \bar{\gamma}_k\big) = 0 \tag{32}$$

is satisfied, which illustrates that the output PDF can track the desired output PDF. That means $\lim_{k\to\infty}(w_g - \bar{w}_k) = 0$, where $\bar{w}_k = \alpha_k D\Delta x_k + \bar{w}_{k-1}$.

The incremental system of the Lipschitz nonlinear dynamic model can be expressed as

$$\begin{cases} \Delta x_{k+1} = A\Delta x_k + B\beta_k\Delta u_k + \Delta g_{xk} + H\Delta f_k + D_0\Delta d_k \\ \bar{w}_k = \alpha_k D\Delta x_k + \bar{w}_{k-1} \end{cases} \tag{33}$$

where $\Delta x_{k+1} = x_{k+1} - x_k$, $\Delta g_{xk} = g(x_k) - g(x_{k-1})$, and $\Delta d_k = d_k - d_{k-1}$.

Define new vectors W_{k+1} and ΔU_k as follows:

$$W_{k+1} = \begin{bmatrix} \bar{w}_{k+1} & \bar{w}_{k+2} & \cdots & \bar{w}_{k+p} \end{bmatrix}^T \tag{34}$$

$$\Delta U_k = \begin{bmatrix} \Delta u_{k|k} & \Delta u_{k+1|k} & \cdots & \Delta u_{k+m-1|k} \end{bmatrix}^T \tag{35}$$

Authorized licensed use limited to: Oak Ridge National Laboratory. Downloaded on August 22,2021 at 17:47:03 UTC from IEEE Xplore. Restrictions apply.

This article has been accepted for inclusion in a future issue of this journal. Content is final as presented, with the exception of pagination.

where p and m are the predictive horizon and the control horizon, respectively. It is worth noting that the condition $p \geq m$ should be satisfied.

The p step prediction of the weight value is formulated as

$$W_{k+1} = S_x \Delta x_k + N\bar{w}_k + S_g \Delta g_{xk} + S_f \Delta f_k + S_d \Delta d_k + S_u \Delta U_k \tag{36}$$

where

$$N = \begin{bmatrix} I_{(n-1)\times(n-1)} & I_{(n-1)\times(n-1)} & \cdots & I_{(n-1)\times(n-1)} \end{bmatrix}^T$$

$$S_x = \begin{bmatrix} \alpha_{k+j}DA & \sum_{j=1}^{2} \alpha_{k+j}DA^j & \cdots & \sum_{j=1}^{p} \alpha_{k+j}DA^j \end{bmatrix}^T$$

$$S_g = \begin{bmatrix} \alpha_{k+j}D & \sum_{j=1}^{2} \alpha_{k+j}DA^{j-1} & \cdots & \sum_{j=1}^{p} \alpha_{k+j}DA^{j-1} \end{bmatrix}^T$$

$$S_f = \begin{bmatrix} \alpha_{k+j}DH & \sum_{j=1}^{2} \alpha_{k+j}DA^{j-1}H & \cdots & \sum_{j=1}^{P} \alpha_{k+j}DA^{j-1}H \end{bmatrix}^T$$

$$S_d = \begin{bmatrix} \alpha_{k+j}DD_0 & \sum_{j=1}^{2} \alpha_{k+j}DA^{j-1}D_0 & \cdots & \sum_{j=1}^{P} \alpha_{k+j}DA^{j-1}D_0 \end{bmatrix}^T$$

$$S_u = \begin{bmatrix} S_{u1} & 0 & 0 & \cdots & 0 \\ \sum_{j=1}^{2} S_{u2} & S_{u3} & 0 & \cdots & 0 \\ \vdots & \vdots & \vdots & \ddots & \vdots \\ \sum_{j=1}^{m} S_{u2} & \sum_{j=1}^{m-1} S_{u4} & \cdots & \cdots & S_{u5} \\ \vdots & \vdots & \vdots & \ddots & \vdots \\ \sum_{j=1}^{p} S_{u2} & \sum_{j=1}^{p-1} S_{u4} & \cdots & \cdots & \sum_{j=1}^{p-m-1} S_{u6} \end{bmatrix}$$

$S_{u1} = \alpha_{k+1}DB\beta_k$, $S_{u2} = \alpha_{k+j}DA^{j-1}B\beta_k$

$S_{u3} = \alpha_{k+1}DB\beta_{k+1}$, $S_{u4} = \alpha_{k+j}DA^{j-1}B\beta_{k+1}$

$S_{u5} = \alpha_{k+1}DB\beta_{k+m-1}$, $S_{u6} = \alpha_{k+j}DA^{j-1}B\beta_{k+m-1}$.

To achieve satisfactory tracking control performance, the following objective function widely used in model predictive control is chosen to guarantee the stability and obtain the optimal control sequence:

$$J = \mathrm{E}\left\{ \sum_{j=1}^{p} \left\| \Gamma_{w,j}\left(\bar{w}_{k+j} - w_g\right) \right\|^2 + \sum_{j=1}^{m} \left\| \Gamma_{u,j} \Delta u_{k+j-1} \right\|^2 \right\} \tag{37}$$

where $\Gamma_{w,j}$ and $\Gamma_{u,j}$ are the jth predictive output error weighting matrix and the jth control input weighting matrix.

Define

$$R_k = W_g - \bar{S}_x \Delta x_k - N\bar{w}_k - \bar{S}_g \Delta g_{xk} - \bar{S}_f \Delta f_k - \bar{S}_d \Delta d_k \tag{38}$$

where

$$W_g = \begin{bmatrix} w_g, & w_g, & , \ldots, & w_g \end{bmatrix}$$

$$\bar{S}_x = \begin{bmatrix} \bar{\alpha}DA & \sum_{j=1}^{2} \bar{\alpha}DA^j & \cdots & \sum_{j=1}^{p} \bar{\alpha}DA^j \end{bmatrix}^T$$

$$\bar{S}_g = \begin{bmatrix} \bar{\alpha}D & \sum_{j=1}^{2} \bar{\alpha}DA^{j-1} & \cdots & \sum_{j=1}^{p} \bar{\alpha}DA^{j-1} \end{bmatrix}^T$$

$$\bar{S}_f = \begin{bmatrix} \bar{\alpha}DH & \sum_{j=1}^{2} \bar{\alpha}DA^{j-1}H & \cdots & \sum_{j=1}^{P} \bar{\alpha}DA^{j-1}H \end{bmatrix}^T$$

$$\bar{S}_d = \begin{bmatrix} \bar{\alpha}DD_0 & \sum_{j=1}^{2} \bar{\alpha}DA^{j-1}D_0 & \cdots & \sum_{j=1}^{P} \bar{\alpha}DA^{j-1}D_0 \end{bmatrix}^T.$$

The objective function is further obtained as

$$\begin{aligned} J &= \left\| \Gamma_w\left(W_{k+1} - W_g\right) \right\|^2 + \left\| \Gamma_u \Delta U_k \right\|^2 \\ &= \begin{bmatrix} \Gamma_w\left(W_{k+1} - W_g\right) \\ \Gamma_u \Delta U_k \end{bmatrix}^T \begin{bmatrix} \Gamma_w\left(W_{k+1} - W_g\right) \\ \Gamma_u \Delta U_k \end{bmatrix} \\ &= \left(\begin{bmatrix} \Gamma_w \bar{S}_u \\ \Gamma_u \end{bmatrix} \Delta U_k - \begin{bmatrix} \Gamma_w R_k \\ 0 \end{bmatrix} \right)^T \\ &\quad \times \left(\begin{bmatrix} \Gamma_w \bar{S}_u \\ \Gamma_u \end{bmatrix} \Delta U_k - \begin{bmatrix} \Gamma_w R_k \\ 0 \end{bmatrix} \right) \end{aligned} \tag{39}$$

where

$$\bar{S}_u = \begin{bmatrix} \bar{S}_{u1} & 0 & 0 & \cdots & 0 \\ \sum_{j=1}^{2} \bar{S}_{u2} & \bar{S}_{u3} & 0 & \cdots & 0 \\ \vdots & \vdots & \vdots & \ddots & \vdots \\ \sum_{j=1}^{m} \bar{S}_{u2} & \sum_{j=1}^{m-1} \bar{S}_{u4} & \cdots & \cdots & \bar{S}_{u5} \\ \vdots & \vdots & \vdots & \ddots & \vdots \\ \sum_{j=1}^{p} \bar{S}_{u2} & \sum_{j=1}^{p-1} \bar{S}_{u4} & \cdots & \cdots & \sum_{j=1}^{p-m-1} \bar{S}_{u6} \end{bmatrix}$$

$\bar{S}_{u1} = \bar{\alpha}DB\bar{\beta}$, $\bar{S}_{u2} = \bar{\alpha}DA^{j-1}B\bar{\beta}$

$\bar{S}_{u3} = \bar{\alpha}DB\bar{\beta}$, $\bar{S}_{u4} = \bar{\alpha}DA^{j-1}B\bar{\beta}$

$\bar{S}_{u5} = \bar{\alpha}DB\bar{\beta}$, $\bar{S}_{u6} = \bar{\alpha}DA^{j-1}B\bar{\beta}$.

The optimal control incremental $\Delta U^*{}_k$ can be obtained by solving $(\partial J/\partial \Delta U_k) = 0$

$$\Delta U^*{}_k = \left(\bar{S}_u^T \Gamma_w^T \Gamma_w \bar{S}_u + \Gamma_u^T \Gamma_u\right)^{-1} \times \bar{S}_u^T \Gamma_w^T \Gamma_w R_k. \tag{40}$$

According to the principle of model predictive control, the first element of $\Delta U^*{}_k$ is chosen as the control incremental signal

$$\Delta u_k = \begin{bmatrix} I_{l\times l} & 0 & \cdots & 0 \end{bmatrix}_{1\times m} \Delta U^*{}_k = K_{mpc} R_k \tag{41}$$

where $K_{mpc} = [I_{l\times l}\, 0 \cdots 0]_{1\times m}(\bar{S}_u^T \Gamma_w^T \Gamma_w \bar{S}_u + \Gamma_u^T \Gamma_u)^{-1} \times \bar{S}_u^T \Gamma_w^T \Gamma_w$ is the predictive control gain.

Remark 4: The matrix Γ_w and the matrix Γ_u should be chosen such that the matrix $\bar{S}_u^T \Gamma_w^T \Gamma_w \bar{S}_u + \Gamma_u^T \Gamma_u$ is invertible, which further ensures the existence of the optimal controller.

Authorized licensed use limited to: Oak Ridge National Laboratory. Downloaded on August 22,2021 at 17:47:03 UTC from IEEE Xplore. Restrictions apply.

This article has been accepted for inclusion in a future issue of this journal. Content is final as presented, with the exception of pagination.

By substituting (41) to (33), the incremental closed-loop system is expressed as follows:

$$\begin{aligned}\Delta x_{k+1} = &\big(A - B\beta_k K_{mpc}(\bar{S}_x + \alpha_k ND)\big)\Delta x_k \\ &+ B\beta_k K_{mpc} W_g + \big(I - B\beta_k K_{mpc}\bar{S}_g\big)\Delta g_{xk} \\ &- BK_{mpc}N\bar{w}_{k-1} + \big(H - B\beta_k K_{mpc}\bar{S}_f\big)\Delta f_k \\ &+ \big(D_0 - B\beta_k K_{mpc}\bar{S}_d\big)\Delta d_k. \end{aligned} \tag{42}$$

System (42) is an interval system and the interval matrix $A' = A - B\beta_k K_{mpc}(\bar{S}_x + \alpha_k ND)$ satisfies the description that $A' \in [\underline{A}', \bar{A}'] = \{A' = [a'_{ij}] \in R^{n\times n} | \underline{a}'_{ij} \le a'_{ij} \le \bar{a}'_{ij}, 1 \le i, j \le n\}$, where $\underline{A}'$ and $\bar{A}'$ are matrices composed of lower and upper bound elements of the interval matrix A'.

Lemma 3 [41]: The interval matrix A' is treated as the following description:

$$A' = A'_0 + E'_0 \Xi F'_0, \quad \Xi \in \Xi^*$$

where

$$\begin{aligned} A'_0 &= \frac{\underline{A}' + \bar{A}'}{2}, H'_0 = \frac{\bar{A}' - \underline{A}'}{2} = \big[h'_{ij}\big] \in R^{n\times n} \\ E'_0 &= \big[\sqrt{h'_{11}} I_1 \cdots \sqrt{h'_{1n}} I_1 \cdots \sqrt{h'_{n1}} I_n \\ &\quad \cdots \quad \sqrt{h'_{nn}} I_n\big] \in R^{n\times n^2} \\ F'_0 &= \big[\sqrt{h'_{11}} I_1 \quad \cdots \quad \sqrt{h'_{1n}} I_n \quad \cdots \quad \sqrt{h'_{n1}} I_1 \\ &\quad \cdots \quad \sqrt{h'_{nn}} I_n\big] \in R^{n^2\times n} \\ \Xi^* &= \Big\{\Xi \in R^{n^2\times n} | \Xi = \mathrm{diag}\big(\big[\varepsilon'_{11}, \ldots, \varepsilon'_{1n}, \ldots, \varepsilon'_{n1} \\ &\qquad \ldots, \varepsilon'_{nn}\big]\big), |\varepsilon'_{ij}| \le 1\Big\}. \end{aligned}$$

I_i is the ith column vector of $I_{n\times n}$.

Theorem 2: Considering the control incremental (41), the incremental control system (42) is stable if the characteristic roots of matrix $A'_0 + E'_0 \Xi F'_0$ are inside the unit circle.

The actual fault-tolerant controller based on the estimated information can be represented as

$$u_k = u_{k-1} + \Delta u_k = u_{k-1} + K_{mpc}\hat{R}_k. \tag{43}$$

The overall control structure diagram for the proposed FTC algorithm is given in Fig. 1. The implementation steps of the FTC algorithm are summarized as follows.

1) Calculate the adaptive gain L and the learning operator Γ by using (21).
2) Formulate $\hat{x}_k$, $\hat{d}_k$, and $\hat{f}_k$ by using (10)–(13).
3) Form the objective function (37).
4) Based on the estimated results, calculate the model predictive fault-tolerant tracking controller u_k by using (43).
5) Apply the acquired fault-tolerant controller u_k to the system when fault occurs.

V. Simulation

A typical papermaking process [7] is used to show the validity of the proposed method, where fibers are considered to be the essential component of the paper, the quality of the paper is often affected by the shape of the fiber length distribution.

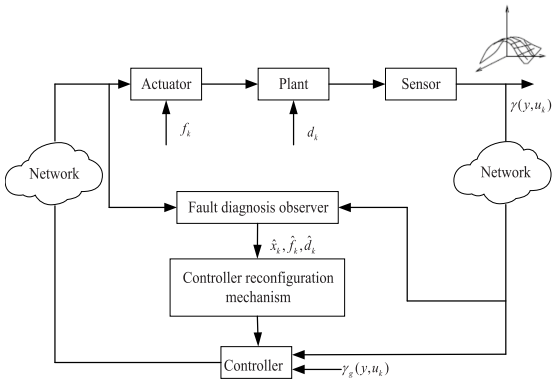

Fig. 1. Diagram of the model predictive fault-tolerant control algorithm.

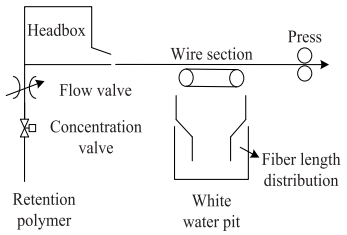

Fig. 2. Diagram of the paper machine wet end.

The following dynamic model of the papermaking process is given:

$$\begin{cases} \theta_{k+1} = -\nu_1\theta_k + \nu_2\mu_k + k_1 u_{1k} \\ \mu_{k+1} = \nu_3\theta_k + (\nu_4 - \nu_2)\mu_k + \nu_5 \sin\theta_k + k_2 u_{2k} \end{cases} \tag{44}$$

where ν_1, ν_2, ν_3, ν_4, and ν_5 are the constants related to the headbox.

u_{1k} and u_{2k} are the flow rate of the retention polymer and the concentration, respectively.

k_1 and k_2 are the constants related to u_{1k} and u_{2k}.

θ_k and μ_k are the shape parameter and the inverse scale parameter, respectively. The PDF of the fiber length distribution can be described as follows:

$$\gamma(y, \theta, \mu) = \Big(\frac{\mu}{\theta}\Big)^{\mu} \frac{y^{\mu-1} e^{-y\mu/\theta}}{\mathrm{G}(\mu)}$$

where $\mathrm{G}(\cdot)$ is the Gamma function. An illustrative diagram of such a system is given in Fig. 2.

Considering the fault caused by the shear force of the headbox approaching system, uncertainties, and the disturbance, the system (44) can be expressed as the discrete-time Lipschitz nonlinear dynamic model (3). Define $x_k = [\theta_k \ \mu_k]^T$ and the coefficient matrices are given as follows:

$$\begin{aligned} A &= \begin{bmatrix} -1.80 & -0.81 \\ 3.44 & 1.10 \end{bmatrix}, B = \begin{bmatrix} -1.5 & 0 \\ 0 & 1.7 \end{bmatrix} \\ F &= \begin{bmatrix} 0.1 \\ 0.2 \end{bmatrix}, H_1 = \begin{bmatrix} 0.02 & 0.01 \end{bmatrix}, H_1 = \begin{bmatrix} 0.01 & 0.01 \end{bmatrix} \\ D &= \begin{bmatrix} 0.2 & 0.1 \\ 0 & 0.1 \end{bmatrix}, H = \begin{bmatrix} -0.5 \\ 1.5 \end{bmatrix}, D_0 = \begin{bmatrix} 0.24 \\ 0.06 \end{bmatrix} \\ C &= \begin{bmatrix} 1 & 0.01 \\ -0.05 & 1 \end{bmatrix}, V = \begin{bmatrix} 1 & 0 \end{bmatrix} \end{aligned}$$

Authorized licensed use limited to: Oak Ridge National Laboratory. Downloaded on August 22,2021 at 17:47:03 UTC from IEEE Xplore. Restrictions apply.

This article has been accepted for inclusion in a future issue of this journal. Content is final as presented, with the exception of pagination.

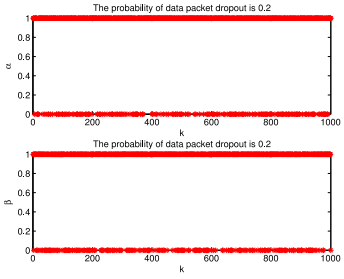

Fig. 3. Packet losses.

$$g(x_k) = \begin{bmatrix} 0 \\ \sin x_{1k} \end{bmatrix}, w_g = \begin{bmatrix} 0.1 \\ 0.5 \end{bmatrix}$$

ϖ_k is the random number on the interval from -1 to 1.

The following functions are selected as the basis functions for approximating the output PDF:

$$\varphi_1(y) = \frac{1}{2}(y-2)^2\chi_1 + \left(-y^2+7y-11.5\right)\chi_2 + \frac{1}{2}(y-5)^2\chi_3$$
$$\varphi_2(y) = \frac{1}{2}(y-3)^2\chi_2 + \left(-y^2+9y-19.5\right)\chi_3 + \frac{1}{2}(y-6)^2\chi_4$$
$$\varphi_3(y) = \frac{1}{2}(y-4)^2\chi_3 + \left(-y^2+11y-29.5\right)\chi_4 + \frac{1}{2}(y-7)^2\chi_5$$

where

$$\chi_s(y) = \begin{cases} 1, & y \in [s+1, s+2] \\ 0, & \text{otherwise} \end{cases} \quad (s = 1, 2, 3, 4, 5).$$

By solving LMI (21), it can be obtained that

$$P_1 = \begin{bmatrix} 0.5881 & 0.3014 & -0.0859 & 0.0024 \\ 0.3014 & 0.1951 & -0.0521 & 0.0016 \\ -0.0859 & -0.0521 & 0.3541 & 0.0084 \\ 0.0024 & 0.0016 & 0.0084 & 0.3372 \end{bmatrix}$$

$$P_2 = \begin{bmatrix} 0.8410 & 0.1576 & -0.0401 & 0.0007 \\ 0.1576 & 0.7579 & -0.0103 & 0.0014 \\ -0.0401 & -0.0103 & 0.5921 & 0.0063 \\ 0.0007 & 0.0014 & 0.0063 & 0.5891 \end{bmatrix}$$

$$P_3 = 6.0583, P_4 = 0.1514$$

$$\Gamma = -5.1, L = \begin{bmatrix} -0.001 & -0.005 & 0.0002 & 0.0004 \end{bmatrix}^T.$$

The additive fault is given as follows:

$$f_k = \begin{cases} 0, & 0 \le k < 300 \\ 2.5, & 300 \le k < 600 \\ 4.5 - 2\exp(-0.3(k-600)), & k \ge 600. \end{cases}$$

The predictive horizon in (34) and the control horizon in (35) are chosen as $p = 4$ and $m = 2$. The matrices Γ_u and Γ_w are chosen, respectively, as

$$\Gamma_u = \text{diag}\{0.1, 0.1, 0.02, 0.01\}$$
$$\Gamma_w = \text{diag}\{0.03, 0.4, 0.6, 0.1, 0.02, 0.3, 0.04, 0.01\}.$$

It can be obtained that the characteristic roots of the incremental system (42) are $-0.4850 + 0.7838i$ and $-0.4850 - 0.7838i$, which are inside the unit circle.

When the probability of packet losses is 0.2, Fig. 3 shows the simulation results of the measurement signal dropouts and the control signal dropouts. Fig. 4 gives the response of the fault and the fault estimation. Fig. 5 gives the response of the system state and the state estimation. The simulation result of the disturbance estimation is shown in Fig. 6. From Figs. 4–6, it indicates that the fault estimation, the system states estimation, and the disturbance estimation can track the change of the fault, the system state, and the disturbance, which lead to satisfactory estimation performance. The output PDF with the proposed fault-tolerant tracking control method is shown in Fig. 7 and the desired output PDF is shown in Fig. 8. Comparing the result of Fig. 7 with that of Fig. 8, it can be seen that the output PDF of the system with the actuator fault can still follow the expected output PDF. This illustrates that the stability and tracking performance of the PDF control system with packet losses can be guaranteed by the proposed fault-tolerant tracking controller. To illustrate the impact of packet losses on the system, the result of fault estimation and the actual output PDF without packet losses compensation are given in Figs. 9 and 10. The effectiveness of the proposed algorithm is further illustrated by Fig. 11, which is the result of the actual output PDF with the presented method in [42].

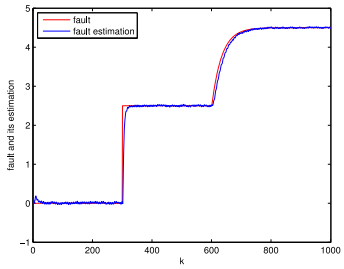

Fig. 4. Fault and fault estimation.

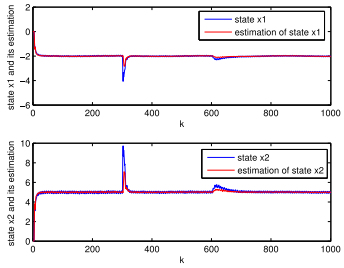

Fig. 5. System state and state estimation.

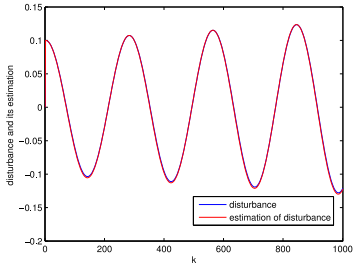

Fig. 6. Disturbance and disturbance estimation.

Remark 5: Packet losses during network transmission will lead to the loss of information including fault characteristics. The results of fault estimation error norm $||\tilde{f}||$ under different

Authorized licensed use limited to: Oak Ridge National Laboratory. Downloaded on August 22,2021 at 17:47:03 UTC from IEEE Xplore. Restrictions apply.

This article has been accepted for inclusion in a future issue of this journal. Content is final as presented, with the exception of pagination.

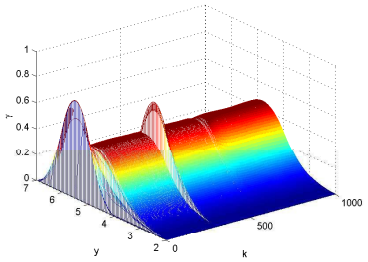

Fig. 7. Actual output PDF with the presented FTC strategy.

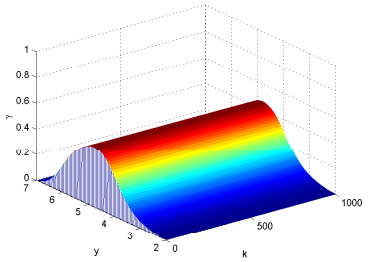

Fig. 8. Desired output PDF.

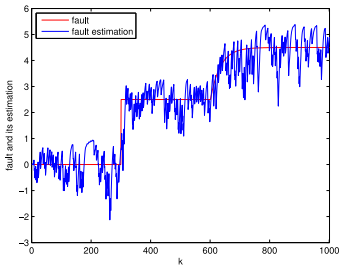

Fig. 9. Result of fault estimation without packet losses compensation.

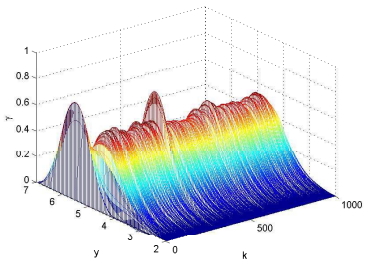

Fig. 10. Actual output PDF without packet losses compensation.

conditions are shown in Table I. It can be seen that with the increase of packet losses rate, the fault estimation error norm remains stable in Case-I and increases rapidly in Case-II. This indicates that packet losses without compensation will make it difficult to accurately estimate the fault information.

Remark 6: The fault whose size changes frequently can also be well estimated by the proposed FD algorithm. The fault is given as follows:

$$f_k = \begin{cases} 0, & 0 \le k < 300 \\ \sin(0.2(k-300)) + 1, & k \ge 300. \end{cases}$$

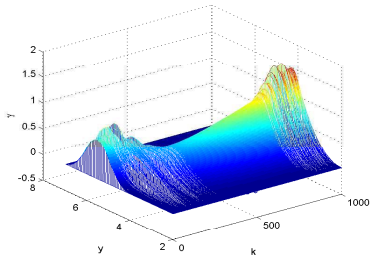

Fig. 11. Actual output PDF with the presented method in [42].

TABLE I
RESULTS OF FAULT ESTIMATION ERROR NORM $||\tilde{f}||$

The probability of packet losses	Case-I	Case-II
0.1	5.0013	13.5233
0.2	5.0035	19.1432
0.3	5.0280	24.2881
0.4	5.0681	40.5056

Case-I: with packet losses compensation
Case-II: without packet losses compensation

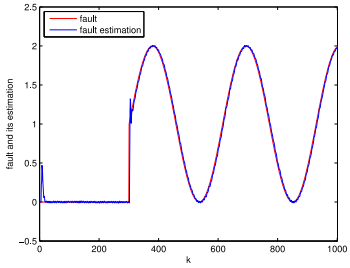

Fig. 12. FD result of the fault with frequent size changes.

The simulation result of the estimation of the fault with frequent size changes is shown in Fig. 12. It can be seen that the trajectory of the fault estimation can well track the change trend of the fault with frequent size changes.

VI. CONCLUSION

An effective fault-tolerant tracking control strategy based on model predictive control is investigated for Lipschitz nonlinear PDF control systems with packet losses in this article. The phenomenon of packet losses is described as the independent Bernoulli distributed white sequences. The proposed fault diagnosis observer can diagnose the fault accurately and timely. Based on the model predictive control principle and the estimated fault information, the control input will be updated in real time to realize the purpose of fault-tolerant tracking control, so that the post-fault system still has the desired tracking performance. Simulation results demonstrate that the presented FTC strategy can effectively guarantee the stability of the system. However, only the additive fault is considered in this article, the design of fault-tolerant controllers for the multiplicative fault and sensor fault [43] remains a challenge. Future work will be devoted to the related research for PDF control systems with packet losses.

Authorized licensed use limited to: Oak Ridge National Laboratory. Downloaded on August 22,2021 at 17:47:03 UTC from IEEE Xplore. Restrictions apply.

This article has been accepted for inclusion in a future issue of this journal. Content is final as presented, with the exception of pagination.

ACKNOWLEDGMENT

The U.S. government retains and the publisher, by accepting the article for publication, acknowledges that the U.S. government retains a nonexclusive, paid-up, irrevocable, worldwide license to publish or reproduce the published form of this manuscript, or allow others to do so, for the U.S. government purposes. DOE will provide public access to these results of federally sponsored research in accordance with the DOE Public Access Plan (http://energy.gov/downloads/doepublic-access-plan).

REFERENCES

[1] T. Li, G. Li, and Q. Zhao, "Adaptive fault-tolerant stochastic shape control with application to particle distribution control," *IEEE Trans. Syst., Man, Cybern., Syst.*, vol. 45, no. 12, pp. 1592–1604, Dec. 2015.

[2] H. Yue, H. Wang, and J. Zhang, "Shaping of molecular weight distribution by iterative learning probability density function control strategies," *Proc. Inst. Mech. Eng. I, J. Syst. Control Eng.*, vol. 222, no. 7, pp. 639–653, 2008.

[3] J. F. Zhang, H. Yue, and J. L. Zhou, "Predictive PDF control in shaping of molecular weight distribution based on a new modeling algorithm," *J. Process Control*, vol. 30, no. 1, pp. 80–89, 2015.

[4] J. L. Zhou, G. T. Li, and H. Wang, "Robust tracking controller design for non-Gaussian singular uncertainty stochastic distribution systems," *Automatica*, vol. 50, no. 4, pp. 1296–1303, 2014.

[5] P. Zhou, M. J. Li, D. W. Guo, H. Wang, and T. Y. Chai, "Modeling for output fiber length distribution of refining process using wavelet neural networks trained by NSGA II and gradient based two-stage hybrid algorithm," *Neurocomputing*, vol. 238, no. 2, pp. 24–32, 2017.

[6] M. J. Li, P. Zhou, H. Wang, and T. Y. Chai, "Geometric analysis based double closed-loop iterative learning control of output PDF shaping of fiber length distribution in refining process," *IEEE Trans. Ind. Electron.*, vol. 66, no. 9, pp. 7229–7238, Sep. 2019.

[7] H. Wang, *Bounded Dynamic Stochastic Systems: Modeling and Control*. London, U.K.: Springer, 2000.

[8] J. L. Zhou, H. Yue, J. F. Zheng, and H. Wang, "Iterative learning double closed-loop structure for modeling and controller design of output stochastic distribution control systems," *IEEE Trans. Control Syst. Technol.*, vol. 22, no. 6, pp. 2261–2276, Nov. 2014.

[9] Y. Wu and J. X. Dong, "Tracking control for non-Gaussian stochastic distribution sampled-data fuzzy systems," *Fuzzy Sets Syst.*, vol. 356, no. 1, pp. 1–27, 2019.

[10] M. F. Ren, Q. C. Zhang, and J. H. Zhang, "An introductory survey of probability density function control," *Syst. Sci. Control Eng.*, vol. 7, no. 1, pp. 158–170, 2019.

[11] L. N. Yao, J. F. Qin, H. Wang, and B. Jiang, "Design of new fault diagnosis and fault tolerant control scheme for non-Gaussian singular stochastic distribution systems," *Automatica*, vol. 48, no. 9, pp. 2305–2313, 2012.

[12] Y. W. Ren, Y. X. Fang, A. P. Wang, H. X. Zhang, and H. Wang, "Collaborative operational fault tolerant control for stochastic distribution control system," *Automatica*, vol. 98, no. 1, pp. 141–149, 2018.

[13] H. K. Jin, Y. C. Guan, and L. N. Yao, "Minimum entropy active fault tolerant control of the non-Gaussian stochastic distribution system subjected to mean constraint," *Entropy*, vol. 19, no. 5, pp. 1–15, 2017.

[14] L. F. Li and L. N. Yao, " Minimum rational entropy fault tolerant control for non-Gaussian singular stochastic distribution control systems using T-S fuzzy modelling," *Int. J. Syst. Sci.*, vol. 49, no. 4, pp. 2900–2911, 2018.

[15] H. J. Gao and T. W. Chen, "H_∞ estimation for uncertain systems with limited communication capacity," *IEEE Trans. Autom. Control*, vol. 52, no. 11, pp. 2070–2084, Nov. 2007.

[16] X.-J. Li and X.-Y. Shen, "A data-driven attack detection approach for DC servo motor systems based on mixed optimization strategy," *IEEE Trans. Ind. Informat.*, vol. 16, no. 9, pp. 5806–5813, Sep. 2020.

[17] Z. K. Ning, J. Y. Yu, Y. N. Pan, and H. Y. Li, "Adaptive event-triggered fault detection for fuzzy stochastic systems with missing measurements," *IEEE Trans. Fuzzy Syst.*, vol. 26, no. 4, pp. 2201–2212, Aug. 2018.

[18] Z. H. Huo, Y. Zheng, and C. Xu, "A robust fault-tolerant control strategy for networked control systems," *J. Netw. Comput. Appl.*, vol. 34, no. 2, pp. 708–714, 2011.

[19] A. B. Qiu, J. P. Gu, C. B. Wen, and J. Zhang, "Self-triggered fault estimation and fault tolerant control for networked control systems," *Neurocomputing*, vol. 272, no. 1, pp. 629–637, 2018.

[20] X. M. Qi and J. S. Qi, "Integrity design for networked control systems with actuator failures and data packet dropouts," *J. Control Sci. Eng.*, vol. 2013, no. 1, pp. 1–9, 2013.

[21] X. G. Yan and C. Edwards, "Nonlinear robust fault reconstruction and estimation using a sliding mode observer," *Automatica*, vol. 43, no. 9, pp. 1605–1614, 2007.

[22] Z. W. Gao, "Fault estimation and fault-tolerant control for discrete-time dynamic systems," *IEEE Trans. Ind. Electron.*, vol. 62, no. 6, pp. 3874–3884, 2015.

[23] J. Han, X. H. Liu, X. W. Gao, and X. J. Wei, "Intermediate observer-based robust distributed fault estimation for nonlinear multiagent systems with directed graphs," *IEEE Trans. Ind. Informat.*, vol. 16, no. 12, pp. 7426–7436, Dec. 2020.

[24] J. Han, H. G. Zhang, Y. C. Wang, and K. Zhang, "Fault estimation and fault-tolerant control for switched fuzzy stochastic systems," *IEEE Trans. Fuzzy Syst.*, vol. 26, no. 5, pp. 2993–3003, Oct. 2018.

[25] L. H. Kong, W. He, C. G. Yang, G. Li, and Z. Q. Zhang, "Adaptive fuzzy control for a marine vessel with time-varying constraints," *IET Control Theory Appl.*, vol. 12, no. 10, pp. 1448–1455, 2018.

[26] L. H. Kong, W. He, C. G. Yang, Z. J. Li, and C. Y. Sun, "Adaptive fuzzy control for coordinated multiple robots with constraint using impedance learning," *IEEE Trans. Cybern.*, vol. 49, no. 8, pp. 3052–3063, Aug. 2019.

[27] B. Xu, C. G. Yang, and Z. K. Shi, "Reinforcement learning output feedback NN control using deterministic learning technique," *IEEE Trans. Neural Netw. Learn. Syst.*, vol. 25, no. 3, pp. 635–641, Mar. 2014.

[28] X. J. Wu and D. H. Gao, "Fault tolerance control of SOFC systems based on nonlinear model predictive control," *Int. J. Hydrogen Energy*, vol. 42, no. 4, pp. 2288–2308, 2017.

[29] J. M. Yu, L. S. Nan, X. M. Tang, and P. Wang, "Model predictive control of non-linear systems over networks with data quantization and packet loss," *ISA Trans.*, vol. 59, no. 1, pp. 1–9, 2015.

[30] R. Q. Lu, Y. Xu, and R. D. Zhang, "A new design of model predictive tracking control for networked control system under random packet loss and uncertainties," *IEEE Trans. Ind. Electron.*, vol. 63, no. 11, pp. 6999–7007, Nov. 2016.

[31] R. Sheikhbahaei, A. Alasty, and J. Vossoughi, "Robust fault tolerant explicit model predictive control," *Automatica*, vol. 97, no. 1, pp. 248–253, 2018.

[32] G. N. Xiao and F. Liu, "Distributed fault-tolerant model predictive control for intermittent fault: A cooperative way," *ISA Trans.*, vol. 89, no. 1, pp. 113–121, 2019.

[33] Y. C. Sun and L. N. Yao, "Robust fault diagnosis and fault-tolerant control for non-Gaussian uncertain stochastic distribution control systems," *Int. J. Robust Nonlinear Control*, vol. 27, no. 10, pp. 1709–1725, 2017.

[34] L. Guo and W. H. Chen, "Disturbance attenuation and rejection for systems with nonlinearity via DOBC approach," *Int. J. Robust Nonlinear Control*, vol. 32, no. 12, pp. 9267–9279, 2005.

[35] A. Isidori and C. I. Byrnes, "Output regulation of nonlinear systems," *IEEE Trans. Autom. Control*, vol. 35, no. 2, pp. 131–140, Feb. 1990.

[36] M. Yang, X. Y. Lang, J. Long, and D. Xu, "Flux immunity robust predictive current control with incremental model and extended state observer for PMSM drive," *IEEE Trans. Power Electron.*, vol. 32, no. 12, pp. 9267–9279, Dec. 2017.

[37] B. Mrugalska, "A bounded-error approach to actuator fault diagnosis and remaining usefullife prognosis of Takagi-Sugeno fuzzy systems," *ISA Trans.*, vol. 80, no. 1, pp. 257–266, 2018.

[38] L. Kong and J. Q. Yuan, "Disturbance-observer-based fuzzy model predictive control for nonlinear processes with disturbances and input constraints," *ISA Trans.*, vol. 90, no. 1, pp. 74–88, 2019.

[39] J. G. Li, J. Q. Yuan, and J. G. Lu, "Observer-based H_∞ control for networked nonlinear systems with random packet losses," *ISA Trans.*, vol. 49, no. 1, pp. 39–46, 2010.

[40] X. Y. Zhang, "Robust integral sliding mode control for uncertain switched systems under arbitrary switching rules," *Nonlinear Anal. Hybrid Syst.*, vol. 37, no. 1, pp. 1–20, 2020.

[41] F. X. Wu, Z. K. Shi, and G. Z. Dai, " On robust stability of dynamic interval systems," *Control Theory Appl.*, vol. 18, no. 1, pp. 113–115, 2001.

[42] L. N. Yao, Z. Y. Yin, and J. F. Qin, "Integrated fault diagnosis and fault tolerant control algorithm for non-Gaussian stochastic distribution systems," *Trans. Beijing Inst. Technol.*, vol. 34, no. 1, pp. 96–101, 2014.

Authorized licensed use limited to: Oak Ridge National Laboratory. Downloaded on August 22,2021 at 17:47:03 UTC from IEEE Xplore. Restrictions apply.

This article has been accepted for inclusion in a future issue of this journal. Content is final as presented, with the exception of pagination.

[43] X.-J. Li and G.-H. Yang, "Fault detection in finite frequency domain for Takagi-Sugeno fuzzy systems with sensor faults," *IEEE Trans. Cybern.*, vol. 44, no. 8, pp. 1446–1458, Aug. 2014.

Lifan Li (Student Member, IEEE) received the B.S. degree in automation from the Zhengzhou University of Light Industry, Zhengzhou, China, in 2015. She is currently pursuing the Ph.D. degree with Zhengzhou University, Zhengzhou.

Her research interests are in fault diagnosis and fault-tolerant control for stochastic distribution systems and nonlinear systems.

Lina Yao (Member, IEEE) received the Ph.D. degree in control theory and control engineering from the Institute of Automation, Chinese Academy of Sciences, Beijing, China, in 2006.

Then, she joined Zhengzhou University, Zhengzhou, China, where she is currently a Professor. From September 2007 to March 2008, she was a Research Fellow with the University of Science and Technology of Lille, Villeneuve-d'Ascq, France. Her research interests are in fault diagnosis and fault-tolerant control for dynamic systems, stochastic distribution control, and flight control.

Hong Wang (Senior Member, IEEE) received the B.S. degree from the Huainan University of Mining Engineering, Huainan, China, in 1982, and the M.S. and Ph.D. degrees in electric drive and its automation from the Huazhong University of Science and Technology, Wuhan, China, in 1984 and 1987, respectively.

He was a Research Fellow with Salford University, Salford, U.K.; Brunel University, Uxbridge, U.K.; and Southampton University, Southampton, U.K. In 1992, he joined the University of Manchester Institute of Science and Technology, Manchester, U.K., where he was a Professor of Process Control from 2002 to 2016. From 2016 to 2018, he was with the Pacific Northwest National Laboratory, Richland, WA, USA, as a Laboratory Fellow and the Chief Scientist, and was the Co-Leader and a Chief Scientist for the Control of Complex Systems Initiative. Since 2019, he has been with the Energy and Transportation Science Division, Oak Ridge National Laboratory, Oak Ridge, TN, USA. His current research interests include stochastic distribution control, fault detection and diagnosis, nonlinear control, and data-based modeling for complex systems. He has authored 200 articles and three books in these research areas.

Dr. Wang was an Associate Editor of the IEEE TRANSACTIONS ON AUTOMATIC CONTROL. He currently serves as an Associate Editor for the IEEE TRANSACTIONS ON CONTROL SYSTEMS TECHNOLOGY and the IEEE TRANSACTIONS ON AUTOMATION SCIENCE AND ENGINEERING.

Authorized licensed use limited to: Oak Ridge National Laboratory. Downloaded on August 22,2021 at 17:47:03 UTC from IEEE Xplore. Restrictions apply.